

000 NEURAL ARCHITECTURE SEARCH BY LEARNING A HI- 001 002 ERARCHICAL SEARCH SPACE 003 004

005 **Anonymous authors**

006 Paper under double-blind review

007 ABSTRACT 008

011 Monte-Carlo Tree Search (MCTS) is a powerful tool for many non-differentiable
012 search related problems such as adversarial games. However, the performance
013 of such approach highly depends on the order of the nodes that are considered at
014 each branching of the tree. If the first branches are not discriminative enough, i.e.
015 they cannot distinguish between promising and deceiving configurations for the
016 final task, the efficiency of the search is exponentially reduced. While in some
017 cases the order of the branching is given as part of the problem (e.g. in chess the
018 sequential order of the moves is defined by the game), in others, such as Neural
019 Architecture Search (NAS), the visiting order of the tree is not important, and only
020 the final architecture matters. **In this paper, we study the application of MCTS to**
021 **NAS for the task of image classification. We analyze several sampling methods and**
022 **branching alternatives for MCTS and propose to learn the branching by hierarchical**
023 **clustering of architectures based on their similarity.** The similarity is measured
024 by the pairwise distance of output vectors of architectures. Extensive experiments
025 on two challenging benchmarks on CIFAR10 and ImageNet show that MCTS, if
026 provided with a good branching hierarchy, can yield promising solutions more
027 efficiently than other approaches for NAS problems.

028 1 INTRODUCTION 029

031 Neural Architecture Search (NAS) aims to automate neural architecture design and has shown great
032 success in the past few years (Zoph & Le, 2016; Real et al., 2019; Liu et al., 2018a; Ren et al., 2021),
033 outperforming manually designed Convolutional Neural Networks (CNN) in deep learning (Liu
034 et al., 2018b; 2019; Guo et al., 2020). NAS aims at yielding the best architecture from a given search
035 space with a lower computational budget than a brute-force approach, based on training all possible
036 architectures independently.

037 One prominent solution is one-shot methods based on weight sharing (Pham et al., 2018), in which
038 multiple architectures share all or part of their weights, eliminating the need for training architectures
039 individually to evaluate their performance. In this approach, a "supernet" that contains all operations/architectures
040 is trained and each architecture is evaluated using weights inherited from that
041 supernet. When architectures are compatible, this approach allows to recycle training iterations (Cha
042 et al., 2022; Pham et al., 2018; Bender et al., 2018); however, when architectures are vastly different,
043 it could lead to interference, i.e the weights that are good for one architecture are detrimental to
044 another and vice-versa (Roshtkhari et al., 2023).

045 To reduce the effect of interference in weight sharing, previous work has used either multiple models
046 that can focus on different parts of the search space (Roshtkhari et al., 2023; Su et al., 2021b; Zhao
047 et al., 2021a; Hu et al., 2022); or importance sampling (Liu et al., 2018b; Ye et al., 2022; Xu et al.,
048 2019) in which the probability of an architecture performing well is estimated during training. In the
049 latter, promising architectures are sampled more frequently during the course of training, gradually
050 reducing the possible interference among architectures (Liu et al., 2018b; You et al., 2020) as the
051 training is guided towards the best architectures. Unlike methods that use uniform sampling for
052 training the supernet (Guo et al., 2020; Roshtkhari et al., 2023), the challenge of using importance
053 sampling is to robustly estimate and identify superior architectures as soon as possible in the training
cycle, to enable the model to focus on them and to avoid wasting training resources on unpromising

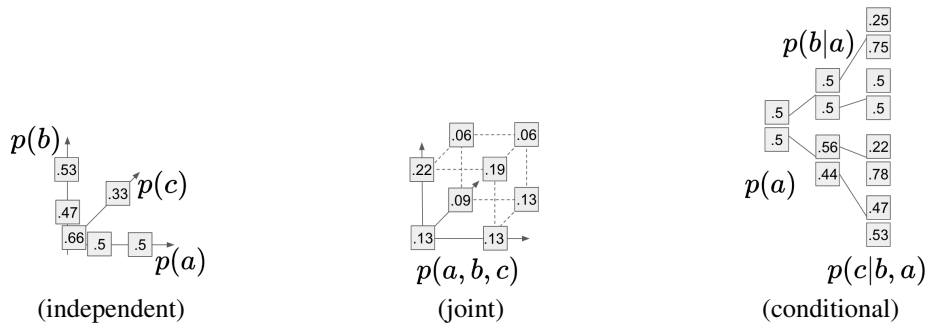


Figure 1: **Probability factorization of 8 architectures.** We show different ways to approximate the discrete probability distribution of architectures for a toy example of search space with $N=3$ nodes (a, b, c in the figure) each one with $O=2$ possible operations for a total of 2^3 architectures. (left) Assuming the nodes independent (as in DARTS (Liu et al., 2018b)) allows the model to estimate only $N \times O$ probabilities. (center) Considering the joint probabilities would require to estimate O^N different probabilities (as in Boltzmann sampling). (right) The joint probability can be factorized into the product of conditional probabilities (in a hierarchy such as in MCTS). This does not reduce the probabilities to estimate, but allows a more efficient exploration of the search space.

architectures. This requires fast and reliable estimation of the probability distribution of architectures in as few training iterations as possible.

A neural network can be considered as a graph, composed of nodes, which define the architecture of the network, connected by edges. These nodes have a choice of operations, which are the actual processes applied to the data (e.g. convolution, fully connected, etc.). In importance sampling, an assumption that makes architecture probability estimation more efficient is "node independence", i.e. considering nodes as statistically independent variables. For instance, in a neural network, the choice of the operation for the second layer would not depend on the choice of the operation in the first layer. As the result, the estimation of an architecture is approximated as the product of nodes' probabilities (see Fig. 1 (independent)). This reduces the scale of the problem to learning individual node probabilities. While the widely used differentiable NAS method (DARTS (Liu et al., 2018b) and followup works (Xu et al., 2019; Li et al., 2020a; Ye et al., 2022)) use this assumption, overlooking the joint contribution of nodes to architecture performance can lead to a poor node selection for the final architecture (Ma et al., 2023).

In order to remove the node independence assumption, the joint probabilities of all configurations should be estimated (see Fig. 1 (joint)). This requires estimating the probability of each architecture independently. Considering mainstream single-path one-shot (SPOS) methods (Guo et al., 2020; Chu et al., 2021b; Li & Talwalkar, 2020; Stamoulis et al., 2019), at each iteration, one architecture from the supernet is sampled, trained and estimated and that estimation is used to update the probability distribution. With node independence, at each iteration several associated node probabilities will be updated, while for joint probabilities only one probability associated with the sampled architecture would be updated. Thus, the full update of the estimation cost proportional to the number of architectures, making it unscalable to large search spaces. Consequently, inefficient estimation of promising architectures slows down the entire training as the importance sampling will not be able to focus on the right architectures.

To explore more wisely, a compelling option is to factorize the joint probability into conditionals, such as a tree used in Monte-Carlo Tree Search (MCTS) (see Fig. 1 (conditional)). While the number of probabilities to estimate do not decrease compared to joint probabilities, this factorization can bring some important advantages. A good hierarchical organization of search space allows more efficient traversal of the tree by reducing the unnecessary exploration of unpromising branches. Prioritizing branches with good solutions can lead to faster convergence, better solution quality and improved scalability. To maximize these advantages, the early nodes of the tree should be highly discriminative. Standard predefined hierarchies of architectures do not guarantee a more efficient exploration, as they are defined by construction and without taking into account the semantic similarity of the corresponding architectures.

108 While in many MCTS problems the searching hierarchy is defined by the sequentiality of the problem
 109 (e.g the moves in chess), for NAS there is no constraint in the order in which the architectures
 110 are explored. Zhao et al. (2021b) and Wang et al. (2021a) leverage this by using the classification
 111 accuracy of the nodes for partitioning the search space into "good" and "bad" nodes to reduce the
 112 unnecessary exploration. This approach works well when running the search with a fixed, already
 113 learned, recognition model (i.e the CNN weights). In fact, Zhao et al. (2021b) uses MCTS for
 114 searching the best performing model on a supernet pre-trained with uniform sampling, while Wang
 115 et al. (2021a) perform MCTS for NAS using the already trained models provided by NAS-Bench-201
 116 (Dong & Yang, 2020).

117 In this work, we tackle the more challenging problem of learning the recognition model and the tree
 118 partitioning jointly. In this setting, at the beginning of the optimization, the recognition model would
 119 have a poor performance, and using its accuracy as proxy to partition the search space would not
 120 work well. We propose instead to estimate the distance between architectures with a partially trained
 121 recognition model in a unsupervised way, without considering the model accuracy. The output vector
 122 of each architecture, sampled from this supernet, is used to calculate a pair-wise distance matrix
 123 of architectures. We propose to use this matrix for hierarchical clustering and generating the tree
 124 partitions. The resulting hierarchical clustering implicitly enforces that the early nodes of tree to be
 125 semantically related, without directly considering their performance. This allows for a better learning
 126 and consequently makes the search faster.

127 The main contributions of our work are the following:

- 128 • We present a new understanding of classical choices of models and approaches for NAS
 129 based on the sampling approach and the estimation of the underlying probability of a given
 130 architecture. We show that too restrictive assumptions (e.g. node independence) allow for
 131 faster training, but converge to worse solutions. Instead, more realistic assumptions could
 132 lead to better solutions if used with some additional regularization.
- 133 • We propose to learn to sample from a MCTS efficiently by learning a good hierarchy that
 134 avoids low performing architectures. We evaluate several approaches to build this hierarchy
 135 and show that the most promising one is obtained through a measure of pairwise distances
 136 among architectures derived from a supernet pre-trained with uniform sampling.
- 137 • We empirically validate our findings on two NAS benchmarks on CIFAR10 dataset and
 138 mobilenet ImageNet search space, showing that the proposed approach is very general and
 139 can find promising architectures within a limited computational budget.

141 2 RELATED WORK

144 **One-shot methods.** One-shot methods (Pham et al., 2018; Bender et al., 2018) has become very
 145 popular in NAS (Liu et al., 2018b; Guo et al., 2020; Su et al., 2021a) due to their efficiency and
 146 flexibility. Generally, the training of supernet and searching for best architecture can be decoupled
 147 (Guo et al., 2020; Wang et al., 2021a) or performed simultaneously (Liu et al., 2018b). In the former,
 148 the search can be performed by various methods, such as random search (Bender et al., 2018; Li &
 149 Talwalkar, 2020), evolutionary algorithms (Guo et al., 2020) or MCTS (Wang et al., 2021a) and the
 150 supernet is static during this phase. The latter alternates between training the supernet and updating
 151 the reward to guide the search, such as updating architecture weights in differentiable methods (Liu
 152 et al., 2018b), controller in RL (Pham et al., 2018) or probability distribution in MCTS (Su et al.,
 153 2021a). The quality of supernet as a proxy for architecture evaluation has been the subject of scrutiny
 154 in recent years, with various results in different settings (Yu et al., 2019; Wang et al., 2021b; Zela
 155 et al., 2019; Termritthikun et al., 2021). A proposed solution is to explicitly reduce the weight
 156 sharing among architectures by non-hierarchical factorization of the search space (Zhao et al., 2021a;
 157 Roshtkhari et al., 2023; Su et al., 2021b). However, in general these methods are computationally
 158 more expensive as they require training additional models. Tree based approaches can be viewed as a
 form of hierarchical factorization of the search space that reduces weight sharing.

159 **Node independence.** While some earlier NAS methods using reinforcement learning (Zoph & Le,
 160 2016; Pham et al., 2018), or evolution (Real et al., 2019; Sun et al., 2020; 2019) do not treat nodes
 161 independently, they were computationally expensive. More efficient and widely used NAS methods
 are differentiable methods (based on DARTS (Liu et al., 2018b)) that use back-propagation to learn

node (architecture) weights (probabilities) alongside supernet weights. However, one of their known problems is that the learned weights of the nodes do not accurately reflect their contribution to the ground truth performance and ranking (Wang et al., 2021b; Yu et al., 2019). While several works has recognized and tried to improve DARTS (Chen et al., 2021c; Ye et al., 2022; Xu et al., 2019), few have directly explored the contribution of node independence assumption to this problem (Ma et al., 2023; Xiao et al., 2022).

Shapley-NAS (Xiao et al., 2022) highlights the underlying relationship between nodes by showing that the joint contribution of node pairs differs from the accumulation of their separate contribution, due to their possible collaboration/competition. They propose reweighing the learned architecture weights by utilizing the Shapley value. However, the estimation of the Shapley value can be costly as it requires training supernet multiple times. ITNAS (Ma et al., 2023) proposes to explicitly model the relationship between the nodes by introducing a transition matrix and an attention vector that denotes the node probability translation to successor nodes. The matrix and vector are optimized in a bi-level framework alongside node probabilities. However, the application of this method is limited to only cell level (inner layer operations) and the application to a more general macro search space is not straightforward (for details about macro and cell-based search spaces see Appendix A). While these works try to incorporate node dependencies into differentiable NAS, an alternative approach is to attempt to directly learn either joint or conditional probabilities of the sampled architectures.

Monte-Carlo Tree Search. MCTS with Upper Confidence bound applied to Trees (UCT) (Auer et al., 2002) has been used previously for NAS (Negrinho & Gordon, 2017; Wistuba, 2017). AlphaX (Wang et al., 2019) used a surrogate network to predict the performance of sample architectures, and MCTS to guide the search. TNAS (Qian et al., 2022) aims to improve the exploration of the search space by using a bi-level tree search that traverses layers and operations iteratively. However, the binary tree that factorizes the operations is manually designed.

LaMOO (Zhao et al., 2021b) and LaNAS (Wang et al., 2021a) aim to tackle the problem of finding the best architecture and assume that deep learning model is given either from a trained supernet (Wang et al., 2021a) or using precomputed benchmarks (Zhao et al., 2021b). In our work instead we aim at training the deep learning model and finding the corresponding optimal architecture with MCTS in the same optimization, which makes the problem more challenging.

The closest work that jointly performs the model training and architecture search with MCTS is Su et al. (2021a) that propose to construct a tree branched along operations. During the training, a hierarchical sampling is used for node selection, updating the supernet weights and the reward (training loss). Node statistics are then used to update a relaxed UCT probability distribution. However, the tree design is manual and a regularization method is required to compensate for insufficient visits of nodes.

3 TRAINING BY SAMPLING ARCHITECTURES

Our training is based on a SPOS (Guo et al., 2020) in which, given a neural model f (e.g. a CNN) for each mini-batch of training data \mathcal{X} and corresponding annotations \mathcal{Y} , a different architecture a from the search space \mathcal{S} is sampled and back-propagated with the following loss:

$$\mathcal{L}(f_a(\mathcal{X}, w), \mathcal{Y}) = \sum_{(x,y) \in (\mathcal{X}, \mathcal{Y})} l(f_a(x, w), y), \quad (1)$$

where l is the loss for a sample (for instance cross-entropy) and w is the network weights. The training speed and model performance can drastically vary depending on how a is sampled. For importance sampling methods, to avoid overfitting on training data, we use validation accuracy as the reward to estimate the probability distribution; and use on-line estimation on mini-batches to accelerate the process. In the following sub-sections, we present some of the most common sampling techniques, from uniform sampling to our proposed approach.

Uniform sampling. This is the simplest and the original approach of SPOS (Guo et al., 2020), in which the architecture is sampled uniformly: $a \sim \mathcal{U}(|\mathcal{S}|)$, where $|\mathcal{S}|$ represents the cardinality of the search space. Although very simple, this sampling is unbiased (does not privilege specific architectures), so that, given enough training, all architectures will have the same importance. This method does not require to store any information during the training, and in principle it can work with

any $|\mathcal{S}|$, even very large ones. In practice however, the equal importance of architectures can lead to two possible problems that hinder the quality of the solution: i) With strong weight sharing (i.e. most of the model weights are shared among all configurations), the same weight would have to adapt to very different architectures, leading to destructive interference and therefore low performance (see Roshtkhari et al. (2023)). ii) If architectures do not share many weights, each is almost independent and the training time would increase proportionally to $|\mathcal{S}|$. While uniform sampling can be combined with search space partitioning to find a trade-off (Roshtkhari et al., 2023), it demands training multiple models, therefore higher memory consumption and computational cost. A different direction is to find ways to prioritize the sampling of the more promising architectures.

Importance sampling with independent probabilities. The simplest way to estimate the importance of each operation is by assuming each node a_i as independent. Thus, the probability of an architecture a is approximated as $p(a) = p(a_1)p(a_2)\dots p(a_t)$. This simplifying assumption allows for a better sampling efficiency by factorizing the number of probabilities to estimate. However, the quality of the solution is decreased, as it disregards the joint influence of nodes on the performance (Ma et al., 2023).

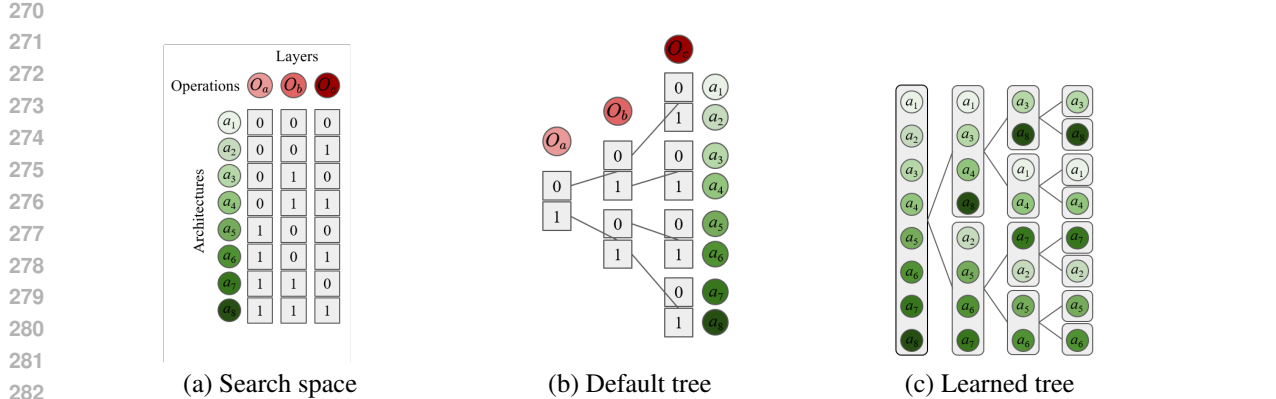
Importance sampling with joint probabilities: Boltzmann sampling. In Boltzmann sampling, architecture a is sampled from a Boltzmann distribution with probability $p(a) \propto \exp(\frac{\epsilon_a}{T})$, where ϵ_a is estimated rewards (here accuracy) of a , and T is the temperature. Sampling is performed with an annealing temperature, starting from a high temperature (almost uniform), such that the initial phase of the training is unbiased, to a low temperature (almost categorical) such that the training focuses on high performing architectures. While more efficient than uniform sampling, estimating ϵ_a is still time consuming, especially for large search spaces and it is difficult to balance exploration/exploitation trade-off in Boltzmann exploration (Cesa-Bianchi et al., 2017).

Sampling with conditional probabilities: **Tree Search.** Instead of considering a flat vector of probabilities, we consider a tree of conditional probabilities: $p(a) = p(a_t|a_{(t' \leq t-1)})p(a_{t-1}|a_{(t' \leq t-2)})\dots p(a_1)$. Each a_t represents a level of the tree and separates the set of possible architectures into disjoint subsets. The commonly used structure of the tree (see Fig.2 (b) Default Tree Structure) is defined by factorizing the model architectures layer by layer (Su et al., 2021a), starting from the first to the last one. Assuming for simplicity a symmetric binary tree, the first level would split the configurations into two disjoint groups, which would be recursively separated into two groups at each following level. With uniform sampling, at each iteration the nodes in level t are sampled with probability $(1/2)^t$. Thus, the estimations of the probabilities of early nodes would be sufficiently accurate because of high sampling rate. In contrast, for Boltzmann, the sampling probability is $1/|\mathcal{S}|$, which can be very small for a large search space. However, if the first nodes maintain a near uniform probability distribution (not discriminative enough), the estimation of the posterior nodes would suffer from low sampling rate. A possible solution is the regularization proposed by Su et al. (2021a), in which at each update of a node, other equivalent nodes (at same level with same operation) are updated similarly with an exponential moving average. This allows for multiple updates simultaneously, that allows for more rapid estimation of probabilities and more efficient exploration.

While this solution seems to work adequately well, this regularization comes with limitations: i) It assumes that the tree is homogeneous at each level, i.e. each node has a similar structure (same children) as others at the same level, which limits the approach to only certain kind of search spaces. For instance, this approach would not work for search spaces in which the operations in a node are conditioned to the choice of operation at the previous node. ii) The assumption of reusing the same probabilities for equivalent nodes, implies treating nodes independently. In this case the node independence assumption is enforced in a soft way by a regularization coefficient. Thus, the method tries to find a compromise between full independence and conditional dependence, but it is unclear if this trade-off is optimal.

4 OUR APPROACH

In our approach, we also tackle the low sampling rate issue in posterior nodes of a MCTS, but from another perspective. We aim to find an ordering of nodes for the tree such that, especially for the first levels of the tree, the probabilities of a sub-node are imbalanced. In this way, the model is able to focus on a reduced set of architectures as the unpromising branches would be estimated early and



283
284
285
286
287
288
289
290
291
292
293
294
295
296
297
298
299
300
301
302
303
304
305
306
307
308
309
310
311
312
313
314
315
316
317
318
319
320
321
322
323

Figure 2: Comparison of the standard tree structure and our learned structure on a 3 binary operations search space. (a) The search space consists of architectures with 3 binary operations (O_a, O_b, O_c) which leads to 8 architectures (a_1, a_2, \dots, a_8). (b) The default tree structure uses the order of operations (e.g. layers) to build the tree, however this is not optimal. (c) Our learned tree structure uses a tree that is generated by an agglomerative clustering on the model outputs.

sampled less frequently. Consider for instance the example in Fig. 1 (conditional): if instead of building the tree from node a , we would start from node c , as the conditional probabilities of c are imbalanced, the model would be able to focus on a good branch more effectively, thus making the sampling much more efficient. This is possible because, in contrast to other problems in which the ordering of nodes is defined as part of the problem, in NAS the final architecture matters and not the order used to reach it. Therefore, in this work we propose to learn an improved ordering of nodes to sample in a MCTS, instead of using a predefined ordering.

Tree design. Consider the toy search space shown in Fig.2(a), with 3 binary operations (O_a, O_b, O_c) which leads to 8 different architectures. The default tree design (Fig. 2(b)) as presented in sec.3, branches off the tree on operation choices per layer. In this section, we present a different approach to build a tree of architectures. As shown in Fig.2 (c), our tree is built as a hierarchical clustering of architectures. Essentially, each node of the tree is a cluster of architectures, going from the root that contains all architectures in a single cluster to the leaves that each contains a single architecture. Through this approach, we release the dependency of the tree from the binary operations and allow any possible hierarchical grouping of configurations. In this work, we build a hierarchy that keeps into account the semantic similarity of among different configurations **A representation of architectures that is independent of the quality of supernet**, while adequately summarizes the relevant information for the task, can be used to determine the placement of architectures in search space. A clustering algorithm can then be used to build the hierarchy based on the difference in distances between architectures. We note that while the ultimate goal of NAS is to find the architecture with highest accuracy, the supernet accuracy is an inadequate representation of architecture for this purpose. The output vector on the other hand, is more suitable as distances between architectures would have semantic meaning in the class space (See sec.5.2 for ablation studies on tree design).

First, a supernet is pre-trained with uniform sampling for a number of iterations. We then sample architectures from the supernet and perform a forward pass with one mini-batch of validation data and record the output vector. The pairwise distances of architectures are calculated and the resulting distance matrix and is used for hierarchical agglomerative clustering (Murtagh & Legendre, 2014) to construct a binary tree. We argue that this method allows us to effectively cluster architectures that have similar overall functionality, even if they might differ in their structure in term of their operations. For more details about the construction of the tree, see algorithm 1 in Appendix B.

Search and training. We use a variation of MCTS for both supernet training and architecture search. Similar to Su et al. (2021a); Wang et al. (2021a), in our case, the tree is already fully expanded and thus expansion and roll-out stages of traditional MCTS are skipped. Similar to Su et al. (2021a), we use Boltzmann sampling for the selection stage. The Boltzmann distribution allows sampling proportional to the probability of the reward function, producing better exploration (Painter et al.,

2024), which is fundamental for a good training of the model. For a node in the tree a_i , we perform importance sampling with a Boltzmann sampling relative to the node:

$$p(a_i) = \frac{\exp(R(a_i)/T)}{\sum_j \exp(R(a_j)/T)}, \quad (2)$$

where R is our reward function and T is temperature, determining the sharpness of distribution and the normalization sum on j is on the sibling nodes of i . Training consists of sampling each level of the tree from the root to the leaf, followed by a gradient update of the recognition model w with the sampled architecture a on a mini-batch of training data \mathcal{X}_{tr} and an update of the reward function for the explored nodes, from the leaf to the root to the tree based on the obtained accuracy of the architecture on a mini-batch of the validation set \mathcal{X}_{val} . To balance exploration/exploitation, we use the Upper Confidence bound applied to Trees (UCT) (Kocsis & Szepesvári, 2006) as reward for sampling. Considering a node in tree a_i , our reward is defined as:

$$R(a_i) = C(a_i) + \lambda \sqrt{\log(|\text{parent}(a_i)|)/|a_i|}, \quad (3)$$

in which the second term is to explore the search space. We use function $|a_i|$ to show number of times node a_i is visited, with the constant λ that controls the exploration/exploitation trade-off. Here, node $\text{parent}(a_i)$ indicates the parent node of a_i . We define C as:

$$C(a_i) = \beta C(a_i) + (1 - \beta) \text{Acc}(f_a(\mathcal{X}_{val}, w)), \quad (4)$$

which is a smoothed version of the validation accuracy for the used architecture a , with smoothing factor β , to account for the noisy on-line estimation on mini-batches. For further details about the training algorithm see algorithm 1 in Appendix B. To search for final architecture after training, we sample k architectures without exploration ($\lambda = 0$) and rank them based on their performance on validation dataset, selecting the best one as final architecture.

5 EXPERIMENTS

In this section, we perform experiments on CIFAR10 dataset (Krizhevsky et al., 2009) using two macro search space benchmarks ,and ImageNet (Russakovsky et al., 2015) with MobielNetV2-like (Sandler et al., 2018) search space . We compare our proposed method with several various sampling methods discussed in sec. 3 (see the summary in Table 6 in Appendix B). In all experiments, we use SPOS method for sampling and training the supernet. For MCTS methods, we start by uniform sampling of the architectures, and after a warm-up period, we use the recorded statistics to calculate UCT (equation 3) and sample using equation 2. Moreover, we initialize $C(a_i) = 1$ to further ensure more exploration at the early stages of training as $C(a_i) < 1$ when nodes are visited. During training, the average accuracy of the supernet will improve, balancing the exploitation/exploration. For MCTS default tree, used by Su et al. (2021a), each layer of CNN is considered as a level of tree, with operations providing the branching and compare the method with and without soft node independence assumption (regularization). For more details on the experiments see Appendix B.

5.1 POOLING SEARCH SPACE

To fully investigate our proposed method, we use Pooling search space, which is a small (36 architectures) but challenging CIFAR10 benchmark with Resnet20 (He et al., 2016) architecture. The only architecture parameter that is searched is feature map sizes at each layer (or equivalently which layer to perform downsamplings). Therefore, at each layer the choices are whether to perform downsampling (pooling operation) or not (Identity operation). The main challenge of this search space is the full weight sharing of architectures that contributes to the inadequacy of several common search methods(Roshtkhari et al., 2023). We represent architectures with number of layers per feature map sizes (e.g. [4,3,3] meaning 4 layers in high resolution, 3 layers middle resolution and 3 layers in low resolution). Our method achieves better results compared to others with similar or less search time (Table 1). For MCTS (default tree design), the regularization proposed in Su et al. (2021a) seems to help, however our method obtains better performance without needing regularization.

378

379 **Table 1: Accuracy and ranking on the Pooling benchmark on CIFAR10.** We report the found
 380 architecture (represented with number of layers per feature map sizes), best and average of 3 training
 381 accuracy and ranking and search time for different methods.

Method	Arch.	Best Acc.	Avg. Acc.	Best Rank	Avg. Rank	Search Time
Default Arch.	[4,3,3]	90.52	-	15	-	-
Uniform	[4,3,3]	90.52	90.40 ± 0.08	15	17	1.5
MCTS	[4,4,2]	90.85	90.57 ± 0.21	12	15.3	2
Boltzmann	[3,5,2]	90.88	90.51 ± 0.12	11	15.3	3
Independent	[3,5,2]	90.88	90.86 ± 0.01	11	11.7	2
Mixtures (Roshtkhari et al., 2023)	[5,3,2]	91.55	91.36 ± 0.27	4	5	6
MCTS + Reg.(Su et al., 2021a)	[6,1,3]	91.78	91.42 ± 0.11	3	3.6	2
MCTS + Learned (ours)	[6,2,2]	91.83	91.72 ± 0.12	2	3	2.2
Best	[7,1,2]	92.01	-	1	-	-

391

392

393 **Table 2: Distance measures for the similarity matrix.** We compare the final performance of our
 394 MCTS with learned tree structure which is built with an agglomerative clustering using a similarity
 395 matrix between network outputs with different distance measures.

Distance Measure	Best Arch.	Best Acc.	Average Accuracy
cross-entropy	[5,3,2]	91.55	91.20 ± 0.23
L2	[6,2,2]	91.83	91.52 ± 0.36
KL	[6,2,2]	91.83	91.72 ± 0.12

401

402 5.2 ABLATION STUDY

403

404 We perform several ablations to study the convergence and performance of our method and investigate
 405 alternative ways to design the hierarchy in Pooling search space.

406

407 **Tree partitioning with accuracy.** We investigate the importance of using the output vector and
 408 clustering to build the tree. For doing that, we build a tree using the accuracy obtained from a
 409 pre-trained supernet, and to recursively partition search space into "good" (top 50% of the partition)
 410 and "bad" regions (bottom 50%). Performing MCTS on this tree, we obtained best and average
 411 accuracy of 90.85% and 90.01% respectively, showing diminished results compared to our method.

412

413 **Clustering distance measures.** We use output of CNN for a mini-batch of data to calculate pairwise
 414 distances. The difference between two distributions can be calculated by several distance measures,
 here we investigate L2 distance, KL divergence, and cross-entropy (Table 2).

415

416 **Supernet training and similarity matrix** During supernet training, the average accuracy of
 417 architectures increases. In our experiments we used supernet at convergence. However, since the
 418 criteria for our proposed clustering is similarity and not the exact accuracy, we only need to train
 419 supernet long enough to capture that similarity. We explore our method with various iterations of
 420 supernet training (see Fig.3(left)). We observe that even without any training, we can still find a
 421 better architecture than the default, and with only 1/3 of full training, we can find better architecture
 422 compared to Roshtkhari et al. (2023). This suggests that we can balance the supernet pertaining
 budget and search budget as the trade-off.

423

424 **Branching quality and NAS convergence.** To show that good branching can speed up NAS, we
 425 compare NAS with our learned tree with default tree and a binary tree created from a random matrix
 426 (see Fig. 3(right)). While the average accuracy of supernet increases in general over epochs, the
 427 branching quality can affect how the search space is explored. After a warm-up period for UCT, our
 428 tree consistently outperforms default and random tree. This suggests that the quality of branching is
 429 important in learning how to explore the search space more efficiently and a low quality hierarchy
 can lead to poor performance.

430

431 **Alternative branching.** While using the output matrix to design the branching is well-performing, it
 requires some initial training of the supernet. We explore using two types of encodings as a zero-cost
 proxy to calculate the similarity matrix. Representing an architecture as a graph, the general encoding

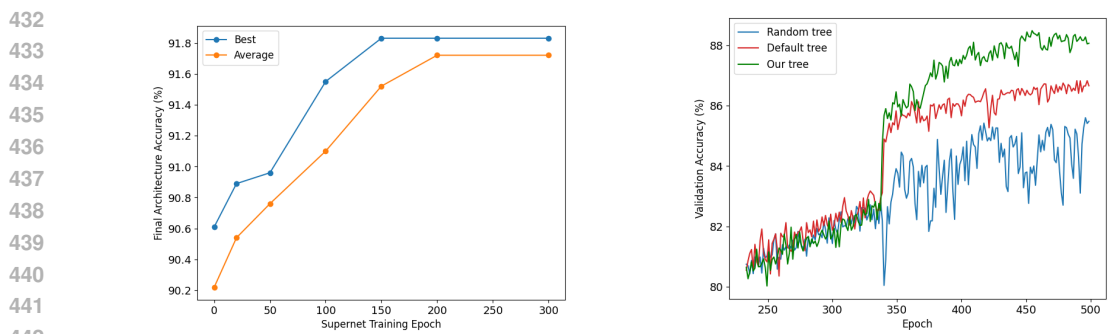


Figure 3: (left) **Training epochs for estimating the similarity matrix.** We show the final performance of our MCTS in which the tree structure is learned with a model uniformly trained for a given number of epochs. For best results at least 200 epochs are needed; (right) **Accuracy over epochs for several training strategies.** After the warm-up phase, our approach is constantly better than default tree or MCTS with a randomly selected tree.

Table 3: **Comparing various zero cost branching methods.** We consider one-hot encoding of operations per layer or the categorical vector representation. The similarity matrix is calculated using L2 distance. We also consider an exponential weighting scheme to increase the influence of earlier layers on distance.

Encoding	Weighting	Best Arch.	Best Acc.	Avg. Acc.
Vector		[2,5,3]	90.89	90.63 ± 0.68
Vector	✓	[3,4,3]	90.92	90.81 ± 0.15
One-hot		[5,2,3]	90.96	90.60 ± 0.22
One-hot	✓	[5,1,4]	91.05	90.78 ± 0.21

is the adjacency matrix, corresponding to the edges (or one-hot encoding of operations per layer). We also consider the categorical representation of the one-hot encoding as vectors as another choice. As shown in Table 3, these two zero-cost encoding techniques do not perform as well as our proposed approach. However, their performance is still better than the most common techniques shown in Table 1. We note that naively calculating the distances (same weight for all layers) is equivalent to considering each layer as an independent variable, while in fact the posterior layers have less importance than early layers. Therefore, we weight each layer l exponentially with $1/2^l$, when calculating the similarity matrix, which leads to slight increases in performance. We hope that in future work it will be possible to learn a good tree structure without pre-training the supernet.

5.3 NAS-BENCH-MACRO SEARCH SPACE

This benchmark based on MobileNetV2 (Sandler et al., 2018) blocks consist of 8 layers and operation set $\{Identity, MB3_K3, MB6_K5\}$ resulting in $3^8 = 6,561$ (3,969 unique) architectures. Table 4 presents results of several sampling based NAS approaches. From the table, we see that our method yields the best architecture of the search space. For each method, we use the best reward and present an ablation on different rewards in Appendix C.1.

5.4 SEARCH ON IMAGENET

ImageNet (Russakovsky et al., 2015) consists of 1.28 million training images in 1000 categories. In our experiments, we use 50k images of validation set as the test data to compare with other methods. To accelerate our training we use mixed precision and FFCV (Leclerc et al., 2023) library. We use similar macro search space to Su et al. (2021a); You et al. (2020); Chu et al. (2021b); Guo et al. (2020), based on MobileNetV2 (Sandler et al., 2018) blocks with optional Squeeze-Excitation (SE) (Hu et al., 2018) module. The total operation choice per layer is 13 resulting in 13^{21} search space size for 21 layers. The choices are convolution kernel size of $\{3, 5, 7\}$ and expansion ratio of $\{3, 6\}$, identity and SE option.

486
 487 **Table 4: Accuracy and ranking on NAS-Bench-Macro.** We compare our method and several
 488 approaches in terms of best, average accuracy and ranking. The architectures are represented with
 489 operation index per layer.

Sampling	Arch.	Best Acc.	Avg. Acc.	Best Rank	Avg. Rank
Boltzmann	[12220111]	92.39	92.30 ± 0.10	406	453
Independent	[22120211]	92.44	92.29 ± 0.21	347	412
MCTS	[22221210]	92.74	92.51 ± 0.18	80	246
Uniform	[21222220]	92.79	92.58 ± 0.20	56	197
MCTS + Reg. (Su et al., 2021a)	[12222222]	92.92	92.67 ± 0.18	21	112
MCTS + Learned (ours)	[22212220]	93.13	92.97 ± 0.12	1	6
Best	[22212220]	93.13	-	1	-

490
 491
 492
 493
 494
 495
 496
 497
 498
 499
 500 **Table 5: Comparison of accuracy and computational cost on ImageNet classification task.** The
 501 architecture are searched on MobilenetV2-based search space. We consider light weight models with
 502 target budget of around 280 MFLOPs. In the top part of the table we report results of other NAS
 503 methods, while at the bottom we report results of our baselines and our approach.

Method	Top-1	Top-5	FLOPs(M)	Params(M)	GPU days
MobileNetV2 1.0 (Sandler et al., 2018)	72.0	91.0	300	3.4	-
MnasNet-A1 (Tan et al., 2019)	75.2	92.5	312	3.9	288
SCARLET-C (Chu et al., 2021a)	75.6	92.6	280	6.0	10
GreedyNAS-C (You et al., 2020)	76.2	92.5	284	4.7	7
MTC_NAS-C (Su et al., 2021a)	76.3	92.6	280	4.9	12
Uniform	72.2	89.7	277	4.6	~ 5
Boltzmann	73.1	89.9	278	4.7	~ 5
MCTS + Reg. (Su et al., 2021a)	76.0	92.6	280	4.9	> 12
MTC + Learned (Ours)	76.3	92.6	280	4.9	~ 7

513
 514 Similar to Su et al. (2021a), we define a FLOPs budget for our search. We leverage the fact that
 515 FLOPs can be used as a zero-cost proxy for architecture performance (Chen et al., 2021b) and search
 516 only within a certain range of target budget ($[0.99, 1] \times \text{budget}$) by sampling architectures and discard
 517 those not within the budget. To compare directly with Su et al. (2021a), we set a budget of 280
 518 MFLOPs. In Table 5.4, we compare our method with several NAS approaches (taken from Su et al.
 519 (2021a)) on the upper part of the table, while we compare with our sampling based approaches on
 520 the bottom part. Note that MCTS + Reg. is our re-implementation of Su et al. (2021a), with some
 521 minor performance differences. Our method yields an architecture that provides high accuracy with
 522 a limited GPU cost. We attribute this advantage to the learned structure of the tree, that allows a
 523 quicker learning of the promising architectures.

525 6 CONCLUSION

526
 527 In this work, we introduce a novel method to design a hierarchical search space for NAS. we highlight
 528 the shortcomings of node independence assumption used in popular NAS methods and the impact of
 529 hierarchical search space design on search quality and efficiency. We show that by simply learning
 530 the proper hierarchy, we can achieve state of the art results with MCTS without requiring further
 531 regularization and established our method empirically the by extensive evaluation on CIFAR10 and
 532 ImageNet.

533 **Limitations** Our proposed method in its current form works best in relatively small ($< 10,000$)
 534 search spaces due to the quadratic complexity of the construction of the pairwise distances for
 535 clustering. Nevertheless, by focusing on a selected budget we were able to tackle much larger search
 536 space as on ImageNet. An analysis of the complexity of our algorithm is provided in Appendix C.5.

537
 538 **Reproducibility Statement** We provide general experimental details in sec. 5 and to further
 539 facilitate the reproducibility of our experiments, we provide necessary implementation detail and
 hyperparameters in Appendix B.

540 REFERENCES
541

- 542 Peter Auer, Nicolo Cesa-Bianchi, and Paul Fischer. Finite-time analysis of the multiarmed bandit
543 problem. *Machine learning*, 47:235–256, 2002.
- 544 Gabriel Bender, Pieter-Jan Kindermans, Barret Zoph, Vijay Vasudevan, and Quoc Le. Understanding
545 and simplifying one-shot architecture search. In *International conference on machine learning*, pp.
546 550–559. PMLR, 2018.
- 547 Nicolò Cesa-Bianchi, Claudio Gentile, Gábor Lugosi, and Gergely Neu. Boltzmann exploration done
548 right. *Advances in neural information processing systems*, 30, 2017.
- 549 Stephen Cha, Taehyeon Kim, Hayeon Lee, and Se-Young Yun. Supernet in neural architecture search:
550 A taxonomic survey. *arXiv preprint arXiv:2204.03916*, 2022.
- 551 Boyu Chen, Peixia Li, Chuming Li, Baopu Li, Lei Bai, Chen Lin, Ming Sun, Junjie Yan, and Wanli
552 Ouyang. Glit: Neural architecture search for global and local image transformer. In *Proceedings
553 of the IEEE/CVF International Conference on Computer Vision*, pp. 12–21, 2021a.
- 554 Hanlin Chen, Ming Lin, Xiuyu Sun, and Hao Li. Nas-bench-zero: A large scale dataset for under-
555 standing zero-shot neural architecture search. 2021b.
- 556 Xin Chen, Lingxi Xie, Jun Wu, and Qi Tian. Progressive darts: Bridging the optimization gap for nas
557 in the wild. *International Journal of Computer Vision*, 129:638–655, 2021c.
- 558 Krishna Teja Chitty-Venkata, Murali Emani, Venkatram Vishwanath, and Arun K Somani. Neural
559 architecture search benchmarks: Insights and survey. *IEEE Access*, 11:25217–25236, 2023.
- 560 Xiangxiang Chu, Bo Zhang, Qingyuan Li, Ruijun Xu, and Xudong Li. Scarlet-nas: bridging the gap
561 between stability and scalability in weight-sharing neural architecture search. In *Proceedings of
562 the IEEE/CVF International Conference on Computer Vision*, pp. 317–325, 2021a.
- 563 Xiangxiang Chu, Bo Zhang, and Ruijun Xu. Fairnas: Rethinking evaluation fairness of weight
564 sharing neural architecture search. In *Proceedings of the IEEE/CVF International Conference on
565 computer vision*, pp. 12239–12248, 2021b.
- 566 Xuanyi Dong and Yi Yang. Nas-bench-201: Extending the scope of reproducible neural architecture
567 search. *arXiv preprint arXiv:2001.00326*, 2020.
- 568 Xuanyi Dong, Lu Liu, Katarzyna Musial, and Bogdan Gabrys. Nats-bench: Benchmarking nas
569 algorithms for architecture topology and size. *IEEE transactions on pattern analysis and machine
570 intelligence*, 44(7):3634–3646, 2021.
- 571 Zichao Guo, Xiangyu Zhang, Haoyuan Mu, Wen Heng, Zechun Liu, Yichen Wei, and Jian Sun.
572 Single path one-shot neural architecture search with uniform sampling. In *Computer Vision–ECCV
573 2020: 16th European Conference, Glasgow, UK, August 23–28, 2020, Proceedings, Part XVI 16*,
574 pp. 544–560. Springer, 2020.
- 575 Kaiming He, Xiangyu Zhang, Shaoqing Ren, and Jian Sun. Deep residual learning for image
576 recognition. In *Proceedings of the IEEE conference on computer vision and pattern recognition*,
577 pp. 770–778, 2016.
- 578 Jie Hu, Li Shen, and Gang Sun. Squeeze-and-excitation networks. In *Proceedings of the IEEE
579 conference on computer vision and pattern recognition*, pp. 7132–7141, 2018.
- 580 Shoukang Hu, Ruochen Wang, Lanqing Hong, Zhenguo Li, Cho-Jui Hsieh, and Jiashi Feng. General-
581 izing few-shot nas with gradient matching. *arXiv preprint arXiv:2203.15207*, 2022.
- 582 Levente Kocsis and Csaba Szepesvári. Bandit based monte-carlo planning. In *European conference
583 on machine learning*, pp. 282–293. Springer, 2006.
- 584 Alex Krizhevsky, Geoffrey Hinton, et al. Learning multiple layers of features from tiny images. 2009.

- 594 Guillaume Leclerc, Andrew Ilyas, Logan Engstrom, Sung Min Park, Hadi Salman, and Aleksander
 595 Madry. FFCV: Accelerating training by removing data bottlenecks. In *Computer Vision and Pattern*
 596 *Recognition (CVPR)*, 2023. <https://github.com/libffcv/ffcv/.commit> xxxxxxxx.
 597
- 598 Guohao Li, Guocheng Qian, Itzel C Delgadillo, Matthias Muller, Ali Thabet, and Bernard Ghanem.
 599 Sgas: Sequential greedy architecture search. In *Proceedings of the IEEE/CVF conference on*
 600 *computer vision and pattern recognition*, pp. 1620–1630, 2020a.
- 601 Jian Li, Yong Liu, Jiankun Liu, and Weiping Wang. Neural architecture optimization with graph vae.
 602 *arXiv preprint arXiv:2006.10310*, 2020b.
- 603 Liam Li and Ameet Talwalkar. Random search and reproducibility for neural architecture search. In
 604 *Uncertainty in artificial intelligence*, pp. 367–377. PMLR, 2020.
- 605
- 606 Chenxi Liu, Barret Zoph, Maxim Neumann, Jonathon Shlens, Wei Hua, Li-Jia Li, Li Fei-Fei, Alan
 607 Yuille, Jonathan Huang, and Kevin Murphy. Progressive neural architecture search. In *Proceedings*
 608 *of the European conference on computer vision (ECCV)*, pp. 19–34, 2018a.
- 609 Chenxi Liu, Liang-Chieh Chen, Florian Schroff, Hartwig Adam, Wei Hua, Alan L Yuille, and Li Fei-
 610 Fei. Auto-deeplab: Hierarchical neural architecture search for semantic image segmentation. In
 611 *Proceedings of the IEEE/CVF conference on computer vision and pattern recognition*, pp. 82–92,
 612 2019.
- 613 Hanxiao Liu, Karen Simonyan, and Yiming Yang. Darts: Differentiable architecture search. *arXiv*
 614 *preprint arXiv:1806.09055*, 2018b.
- 615
- 616 Jovita Lukasik, David Friede, Arber Zela, Frank Hutter, and Margret Keuper. Smooth variational
 617 graph embeddings for efficient neural architecture search. In *2021 International Joint Conference*
 618 *on Neural Networks (IJCNN)*, pp. 1–8. IEEE, 2021.
- 619 Jovita Lukasik, Steffen Jung, and Margret Keuper. Learning where to look—generative nas is
 620 surprisingly efficient. In *European Conference on Computer Vision*, pp. 257–273. Springer, 2022.
- 621
- 622 Benteng Ma, Jing Zhang, Yong Xia, and Dacheng Tao. Inter-layer transition in neural architecture
 623 search. *Pattern Recognition*, 143:109697, 2023.
- 624 Fionn Murtagh and Pierre Legendre. Ward’s hierarchical agglomerative clustering method: which
 625 algorithms implement ward’s criterion? *Journal of classification*, 31:274–295, 2014.
- 626
- 627 Renato Negrinho and Geoff Gordon. Deeparchitect: Automatically designing and training deep
 628 architectures. *arXiv preprint arXiv:1704.08792*, 2017.
- 629
- 630 Xuefei Ning, Yin Zheng, Tianchen Zhao, Yu Wang, and Huazhong Yang. A generic graph-based
 631 neural architecture encoding scheme for predictor-based nas. In *European Conference on Computer*
 632 *Vision*, pp. 189–204. Springer, 2020.
- 633
- 634 Michael Painter, Mohamed Baioumy, Nick Hawes, and Bruno Lacerda. Monte carlo tree search with
 boltzmann exploration. *Advances in Neural Information Processing Systems*, 36, 2024.
- 635
- 636 Hieu Pham, Melody Guan, Barret Zoph, Quoc Le, and Jeff Dean. Efficient neural architecture search
 via parameters sharing. In *International conference on machine learning*, pp. 4095–4104. PMLR,
 637 2018.
- 638
- 639 Guocheng Qian, Xuanyang Zhang, Guohao Li, Chen Zhao, Yukang Chen, Xiangyu Zhang, Bernard
 Ghanem, and Jian Sun. When nas meets trees: An efficient algorithm for neural architecture search.
 640 In *Proceedings of the IEEE/CVF Conference on Computer Vision and Pattern Recognition*, pp.
 641 2782–2787, 2022.
- 642
- 643 Esteban Real, Alok Aggarwal, Yanping Huang, and Quoc V Le. Regularized evolution for image
 644 classifier architecture search. In *Proceedings of the aaai conference on artificial intelligence*,
 645 volume 33, pp. 4780–4789, 2019.
- 646
- 647 Pengzhen Ren, Yun Xiao, Xiaojun Chang, Po-Yao Huang, Zhihui Li, Xiaojiang Chen, and Xin Wang.
 A comprehensive survey of neural architecture search: Challenges and solutions. *ACM Computing*
Surveys (CSUR), 54(4):1–34, 2021.

- 648 Mehraveh Javan Roshtkhari, Matthew Toews, and Marco Pedersoli. Balanced mixture of supernets
 649 for learning the cnn pooling architecture. In *International Conference on Automated Machine*
 650 *Learning*, pp. 8–1. PMLR, 2023.
- 651
- 652 Olga Russakovsky, Jia Deng, Hao Su, Jonathan Krause, Sanjeev Satheesh, Sean Ma, Zhiheng Huang,
 653 Andrej Karpathy, Aditya Khosla, Michael Bernstein, Alexander C. Berg, and Li Fei-Fei. ImageNet
 654 Large Scale Visual Recognition Challenge. *International Journal of Computer Vision (IJCV)*, 115
 655 (3):211–252, 2015. doi: 10.1007/s11263-015-0816-y.
- 656
- 657 Mark Sandler, Andrew Howard, Menglong Zhu, Andrey Zhmoginov, and Liang-Chieh Chen. Mo-
 658 bilenetv2: Inverted residuals and linear bottlenecks. In *Proceedings of the IEEE conference on*
659 computer vision and pattern recognition, pp. 4510–4520, 2018.
- 660
- 661 Julien Siems, Lucas Zimmer, Arber Zela, Jovita Lukasik, Margret Keuper, and Frank Hutter. Nas-
 662 bench-301 and the case for surrogate benchmarks for neural architecture search. *arXiv preprint*
663 arXiv:2008.09777, 11, 2020.
- 664
- 665 Dimitrios Stamoulis, Ruizhou Ding, Di Wang, Dimitrios Lymberopoulos, Bodhi Priyantha, Jie Liu,
 666 and Diana Marculescu. Single-path nas: Designing hardware-efficient convnets in less than 4 hours.
 667 In *Joint European Conference on Machine Learning and Knowledge Discovery in Databases*, pp.
 668 481–497. Springer, 2019.
- 669
- 670 Xiu Su, Tao Huang, Yanxi Li, Shan You, Fei Wang, Chen Qian, Changshui Zhang, and Chang Xu.
 Prioritized architecture sampling with monto-carlo tree search. In *Proceedings of the IEEE/CVF*
671 Conference on Computer Vision and Pattern Recognition, pp. 10968–10977, 2021a.
- 672
- 673 Xiu Su, Shan You, Mingkai Zheng, Fei Wang, Chen Qian, Changshui Zhang, and Chang Xu. K-shot
 674 nas: Learnable weight-sharing for nas with k-shot supernets. In *International Conference on*
Machine Learning, pp. 9880–9890. PMLR, 2021b.
- 675
- 676 Yanan Sun, Bing Xue, Mengjie Zhang, and Gary G Yen. Evolving deep convolutional neural networks
 for image classification. *IEEE Transactions on Evolutionary Computation*, 24(2):394–407, 2019.
- 677
- 678 Yanan Sun, Bing Xue, Mengjie Zhang, Gary G Yen, and Jiancheng Lv. Automatically designing
 679 cnn architectures using the genetic algorithm for image classification. *IEEE transactions on*
cybernetics, 50(9):3840–3854, 2020.
- 680
- 681 Mingxing Tan, Bo Chen, Ruoming Pang, Vijay Vasudevan, Mark Sandler, Andrew Howard, and
 682 Quoc V Le. Mnasnet: Platform-aware neural architecture search for mobile. In *Proceedings of the*
683 IEEE/CVF conference on computer vision and pattern recognition, pp. 2820–2828, 2019.
- 684
- 685 Chakkrit Termritthikun, Yesi Jamtsho, Jirarat Ieamsaard, Paisarn Muneesawang, and Ivan Lee.
 Eeea-net: An early exit evolutionary neural architecture search. *Engineering Applications of*
686 Artificial Intelligence, 104:104397, 2021.
- 687
- 688 Linnan Wang, Yiyang Zhao, Yuu Jinnai, Yuandong Tian, and Rodrigo Fonseca. Alphax: exploring
 689 neural architectures with deep neural networks and monte carlo tree search. *arXiv preprint*
690 arXiv:1903.11059, 2019.
- 691
- 692 Linnan Wang, Saining Xie, Teng Li, Rodrigo Fonseca, and Yuandong Tian. Sample-efficient neural
 693 architecture search by learning actions for monte carlo tree search. *IEEE Transactions on Pattern*
694 Analysis and Machine Intelligence, 44(9):5503–5515, 2021a.
- 695
- 696 Ruochen Wang, Minhao Cheng, Xiangning Chen, Xiaocheng Tang, and Cho-Jui Hsieh. Rethinking
 697 architecture selection in differentiable nas. *arXiv preprint arXiv:2108.04392*, 2021b.
- 698
- 699 Colin White, Willie Neiswanger, Sam Nolen, and Yash Savani. A study on encodings for neural
 700 architecture search. *Advances in neural information processing systems*, 33:20309–20319, 2020.
- 701
- Colin White, Willie Neiswanger, and Yash Savani. Bananas: Bayesian optimization with neural
 architectures for neural architecture search. In *Proceedings of the AAAI Conference on Artificial*
Intelligence, volume 35, pp. 10293–10301, 2021.

- 702 Colin White, Mahmoud Safari, Rhea Sukthanker, Binxin Ru, Thomas Elsken, Arber Zela, Debadatta
 703 Dey, and Frank Hutter. Neural architecture search: Insights from 1000 papers. *arXiv preprint*
 704 *arXiv:2301.08727*, 2023.
- 705 Martin Wistuba. Finding competitive network architectures within a day using uct. *arXiv preprint*
 706 *arXiv:1712.07420*, 2017.
- 708 Han Xiao, Ziwei Wang, Zheng Zhu, Jie Zhou, and Jiwen Lu. Shapley-nas: discovering operation
 709 contribution for neural architecture search. In *Proceedings of the IEEE/CVF conference on*
 710 *computer vision and pattern recognition*, pp. 11892–11901, 2022.
- 711 Yuhui Xu, Lingxi Xie, Xiaopeng Zhang, Xin Chen, Guo-Jun Qi, Qi Tian, and Hongkai Xiong.
 712 Pc-darts: Partial channel connections for memory-efficient architecture search. *arXiv preprint*
 713 *arXiv:1907.05737*, 2019.
- 715 Shen Yan, Yu Zheng, Wei Ao, Xiao Zeng, and Mi Zhang. Does unsupervised architecture representa-
 716 tion learning help neural architecture search? *Advances in neural information processing systems*,
 717 33:12486–12498, 2020.
- 718 Shen Yan, Kaiqiang Song, Fei Liu, and Mi Zhang. Cate: Computation-aware neural architecture
 719 encoding with transformers. In *International Conference on Machine Learning*, pp. 11670–11681.
 720 PMLR, 2021.
- 722 Peng Ye, Baopu Li, Yikang Li, Tao Chen, Jiayuan Fan, and Wanli Ouyang. b-darts: Beta-decay
 723 regularization for differentiable architecture search. In *proceedings of the IEEE/CVF conference*
 724 *on computer vision and pattern recognition*, pp. 10874–10883, 2022.
- 725 Chris Ying, Aaron Klein, Eric Christiansen, Esteban Real, Kevin Murphy, and Frank Hutter. Nas-
 726 bench-101: Towards reproducible neural architecture search. In *International conference on*
 727 *machine learning*, pp. 7105–7114. PMLR, 2019.
- 729 Shan You, Tao Huang, Mingmin Yang, Fei Wang, Chen Qian, and Changshui Zhang. Greedynas:
 730 Towards fast one-shot nas with greedy supernet. In *Proceedings of the IEEE/CVF Conference on*
 731 *Computer Vision and Pattern Recognition*, pp. 1999–2008, 2020.
- 732 Kaicheng Yu, Christian Sciuto, Martin Jaggi, Claudiu Musat, and Mathieu Salzmann. Evaluating the
 733 search phase of neural architecture search. *arXiv preprint arXiv:1902.08142*, 2019.
- 735 Arber Zela, Thomas Elsken, Tonmoy Saikia, Yassine Marrakchi, Thomas Brox, and Frank Hutter. Un-
 736 derstanding and robustifying differentiable architecture search. *arXiv preprint arXiv:1909.09656*,
 737 2019.
- 738 Muhan Zhang, Shali Jiang, Zhicheng Cui, Roman Garnett, and Yixin Chen. D-vae: A variational
 739 autoencoder for directed acyclic graphs. *Advances in Neural Information Processing Systems*, 32,
 740 2019.
- 741 Yiyang Zhao, Linnan Wang, Yuandong Tian, Rodrigo Fonseca, and Tian Guo. Few-shot neural
 742 architecture search. In *International Conference on Machine Learning*, pp. 12707–12718. PMLR,
 743 2021a.
- 745 Yiyang Zhao, Linnan Wang, Kevin Yang, Tianjun Zhang, Tian Guo, and Yuandong Tian. Multi-
 746 objective optimization by learning space partitions. *arXiv preprint arXiv:2110.03173*, 2021b.
- 747 Barret Zoph and Quoc V Le. Neural architecture search with reinforcement learning. *arXiv preprint*
 748 *arXiv:1611.01578*, 2016.
- 750 Barret Zoph, Vijay Vasudevan, Jonathon Shlens, and Quoc V Le. Learning transferable architectures
 751 for scalable image recognition. In *Proceedings of the IEEE conference on computer vision and*
 752 *pattern recognition*, pp. 8697–8710, 2018.
- 753
- 754
- 755

756 **A MORE RELATED WORK**
 757

758 **Search space design** Common NAS search spaces can be categorized as Micro (cell-based), Macro,
 759 and mulit-level. Micro search spaces (Zoph et al., 2018; Liu et al., 2018b) focus on yielding the
 760 optimal architecture by finding the operations that can produce the best model inside a cell or block.
 761 The cell is then stacked to form the entire network, while the outer skeleton of the network is often
 762 controlled manually by including reduction cells. This was inspired by observing that the state-of-
 763 the-art manual architectures were formed by repetition of a certain structure and helped to reduce the
 764 complexity of search space to a manageable level (White et al., 2023).

765 Therefore, the objective of this approach is to find a cell that works well on all parts of the network,
 766 which might be suboptimal. This neglects to explore non-homogeneous architectures and diminishes
 767 the capability of NAS to find novel architectures. Macro search space (Su et al., 2021a) instead
 768 searches for the outer skeleton of the network while fixing the operations at micro level. This can
 769 include architecture parameters such as: type of layers, number of layers, or channels in layers,
 770 pooling positions etc. Finally, a mulit-level search space searches at two levels: cell and macro
 771 structure for a CNN (Liu et al., 2019) or convolution and self-attention layers for vision transformers
 772 (Chen et al., 2021a). In this work, we focus on macro search spaces as it is generally more expressive
 773 and challenging than micro search spaces.

774 **NAS benchmarks** NAS benchmarks are used to evaluate for a given method the quality and the
 775 amount of computation required to yield a solution. They have played a crucial role in the NAS
 776 community as they provide an evaluation of all architectures in a brute-force way to find the optimal
 777 solution and eliminate the need to run independently this expensive process. The development of
 778 NAS benchmarks has also improved the reproducibility and efficiency of NAS research. Tabular
 779 benchmarks (Ying et al., 2019; Su et al., 2021a) are constructed by exhaustively training and evaluating
 780 (metrics such as accuracy, FLOPS, number of parameters, etc.) all possible architectures. On the
 781 other hand, surrogate benchmarks (Siems et al., 2020) estimate the architecture performance using a
 782 model which is trained on data from several trained architectures. Benchmarks have been developed
 783 for both micro (Ying et al., 2019; Dong & Yang, 2020; Siems et al., 2020) (with addition of channels
 784 (Dong et al., 2021)) and macro (Su et al., 2021a; Roshtkhari et al., 2023) search spaces. For more
 785 details on NAS benchmarks see the survey Chitty-Venkata et al. (2023).

786 **Architecture encoding** Some works have shown that architecture encoding can affect the perfor-
 787 mance of NAS (White et al., 2020; Ying et al., 2019) and good encoding of architectures enables
 788 efficient calculation of relationships or distances among architectures. The most common encoding
 789 represents the architecture as a directed acyclic graph (DAG) and adjacency matrix along with a list
 790 of operations (Ying et al., 2019; Zoph & Le, 2016). For using performance predictors, BANANAS
 791 (White et al., 2021) proposes a path-based encoding instead of adjacency matrix and GATES (Ning
 792 et al., 2020) proposed a graph based encoding scheme that better mode the flow information in the
 793 network. Encoding can also be learned by unsupervised training prior to NAS often utilizing an
 794 autoencoder (Li et al., 2020b; Lukasik et al., 2021; 2022; Yan et al., 2020; Zhang et al., 2019) or a
 795 transformer (Yan et al., 2021). In our work, we make use and compare different ways of encoding
 796 architectures for our approach as ablation and show that measuring distances based on the network
 797 output seems to be the fundamental for good results.

798 **B EXPERIMENTAL SETUP AND DETAILS**
 799

800 **Sampling method details** A summary of various methods used in our experiments (Tables 1 and 4)
 801 is presented in Table 6.

802 **Training Algorithm** The training pipeline for our method is shown in algorithm 1. First, a pre-
 803 training with random sampling of the architectures is performed in order to train an initial model
 804 f with parameters w_p . With this model we build a pairwise matrix $D_{i,j}$ that measures the distance
 805 of configuration i and j on the output space of the model. With this matrix, we use agglomerative
 806 clustering to build a binary tree that represents the hierarchy that will be used for the subsequent
 807 MCTS training. During training, an architecture is sampled from the tree, where at each node
 808 Boltzmann sampling with the learned probabilities is used. Then, this architecture is used to update
 809

Method	Search Space Structure	Sampling Method
Uniform	Flat	Uniform (sec. 3)
Independent	Flat	Nodes sampled independently (sec. 3)
Boltzmann	Flat	Joint prob. (sec. 3)
Mixture	Flat (partitioned)	Uniform (Roshtkhari et al., 2023)
MCTS	Hierarchical (def. tree)	Conditional prob. (sec. 3, Tree Search)
MCTS + Reg.	Hierarchical (def. tree)	Conditional prob. + regularization (Su et al., 2021a)
MCTS + Learned	Hierarchical (learned tree)	Conditional prob. (sec. 4)

the model on a mini-batch of training data (for simplicity we did not include momentum in the gradient updates) and to estimate its accuracy on a validation mini-batch. The validation accuracy is smoothed with an exponential moving average and used as reward with UCT regularization for updating the node probabilities of the sampled architecture. Finally, after the MCTS, the best architectures are sampled from the tree by sampling the tree with $\lambda = 0$.

Algorithm 1: Simplified pseudo-code of our training pipeline.

Input : \mathcal{S} : Search Space; $\mathcal{X}_t, \mathcal{X}_v$: mini-batches of training and validation data; f_a : model with architecture a ; w_p, w : weights of the pre-trained and final model initialized randomly; e_{pt}, e_{MCTS} : pre-training and MCTS iterations; α : learning rate; β : smoothing factor; λ : exploration parameter of UCT.

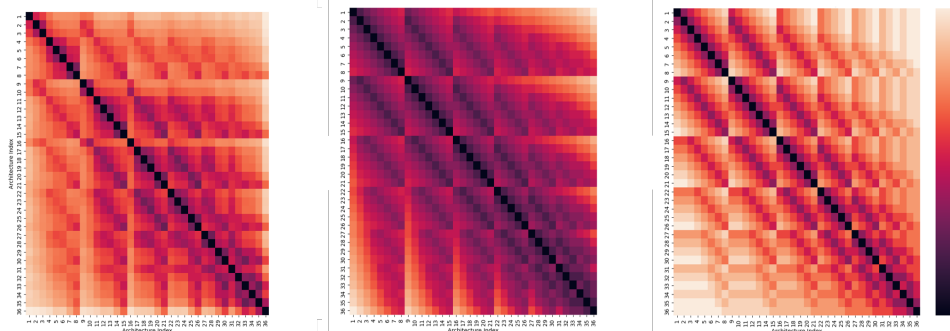
```

#pre-training
while epochs ≤ ept do
    | a ← sample from  $\mathcal{U}(|\mathcal{S}|)$ 
    | wp ← wp − α∇wp  $\mathcal{L}(f_a(\mathcal{X}_t, w_p))$ 
end
#build the search tree
for ai ∈  $\mathcal{S}$  do
    | Output vector oi ← fai( $\mathcal{X}_v, w_p$ )
end
Distance matrix Dij = dist(oi, oj)
Binary tree  $\mathcal{T}$  ← aggl_clustering(D)
#main training with MCTS
while epochs ≤ eMCTS do
    #sample an architecture a
    a = []
    node = "root"
    push(a, node)
    while not(is_leaf(node)) do
        | node ← sample(next(node)) with Boltzmann sampling as in Eq.(2)
        | push(a, node)
    end
    #update model w and accuracy
    w ← w − α∇w  $\mathcal{L}(f_a(\mathcal{X}_t, w))$ 
    accuracy ← Acc(fa( $\mathcal{X}_{val}, w$ ))
    node ← pop(a)
    #update rewards
    while not(is_root(node)) do
        | parent ← pop(a)
        | C(node) ← β C(node) + (1 − β) accuracy
        | R(node) ← C(node) + λ  $\sqrt{\log(|parent|)/|node|}$ 
        | node ← parent
    end
end
Output : Best architecture from  $\mathcal{T}$  by sampling with  $\lambda = 0$ 

```

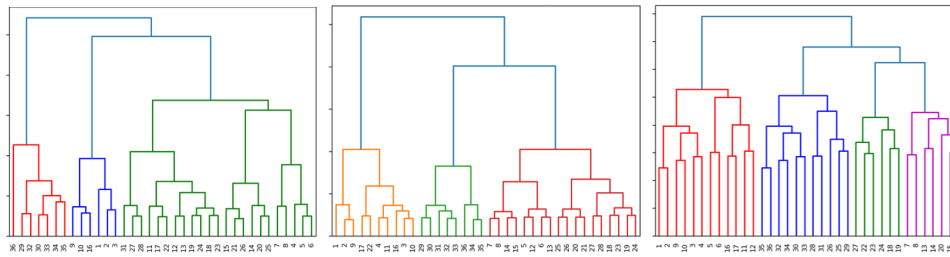
864 **B.1 DATASET AND HYPERPARAMETES**
 865
 866 For experiments performed on CIFAR10 (Kocsis & Szepesvari, 2006) dataset, we split the training
 867 set 50/50 for NAS training and validation. To tune hyperparameters, we either performed grid search
 868 or when comparing with other works used similar hyperparameters. We used SGD with weight
 869 decay and cosine annealing learning rate schedule. Furthermore, for MCTS methods we split training
 870 iterations to roughly 40/25/35 fractions for uniform sampling/MCTS warm-up/MCTS sampling
 871 respectively. In all experiments we use $\beta = 0.95$ and $\lambda = 0.5$.
 872
 873 **Pooling search space** This search space introduced by Roshtkhari et al. (2023) is based on Resnet20
 874 (He et al., 2016) architecture. The only CNN parameters to search is where to perform pooling. To
 875 calculate distance matrix we trained the supernet for 300 epoch using uniform sampling with batch
 876 size 512, learning rate 0.1 and weight decay 1e-3. For search we trained for 400 epochs with batch
 877 size 256, learning rate learning rate 0.05 and temperature T is set to linearly annealing schedule (0.02,
 878 0.0025). Since this search space is small we only consider nodes with max probabilities and report
 879 the it as the final architecture.
 880
 881 **NAS-Bench-Macro search space** This benchmark introduced by Su et al. (2021a) is based on
 882 MobileNetV2 (Sandler et al., 2018) blocks. The supernet pre-training is performed for 80 epochs
 883 with batch size 512 and learning rate 0.05. For search we use batch size of 256 for 120 epochs with
 884 and T linearly annealing from 0.01. At the ends of training, we sample 50 architectures from the tree
 885 and report the best as final architecture.
 886
 887 **ImageNet** To accelerate our training in ImageNet experiments, we use mixed precision and FFCV
 888 (Leclerc et al., 2023) library. We sample architectures within a FLOPs budget and discard those
 889 outside of it. We train for 100 epochs with SGD and cosine annealing learning rate. Other training
 890 strategies are similar to experiments on CIFAR10.
 891
 892 **C ADDITIONAL RESULTS**
 893
 894 **C.1 REWARD FOR MCTS**
 895
 896 The most common rewards used for NAS algorithms is accuracy and loss. While loss is differentiable,
 897 accuracy is more aligned with the objective of NAS. Furthermore, either the training or validation
 898 can be used to calculate the reward. Instead of absolute values, a relative training loss metric was
 899 used in Su et al. (2021a) to account for unfair reward comparison at different iteration of supernet
 900 training. In Table 7 for NAS-Bench-Macro, we explore some common combination of options to
 901 estimate the reward. In all setting our approach performs on par or slightly better than Default Tree
 902 + Regularization. For both methods it seems that using the accuracy on the validation set as metric
 903 is the best. However, while for our approach the best performing configuration is obtained with the
 904 absolute metric, for Su et al. (2021a) the relative metric seems slightly better.
 905
 906 **C.2 DISTANCE MATRICES**
 907
 908 We visualize the distance matrices calculated using output vector and various encoding in Fig. 4.
 909
 910 **C.3 TREE VISUALIZATIONS**
 911
 912 For pooling search space, we visualize tree structure based on our proposed method and architecture
 913 encodings in Fig. 5. The tree is presented with architecture indices on leaves. The architecture indices
 914 and the corresponding performance can be found in Roshtkhari et al. (2023).
 915
 916 **C.4 ARCHITECTURE VISUALIZATION**
 917
 We show the found architecture by our method for ImageNet in Fig. 6.

918
919
920
921
922
923
924
925
926
927
928
929
930
931
932



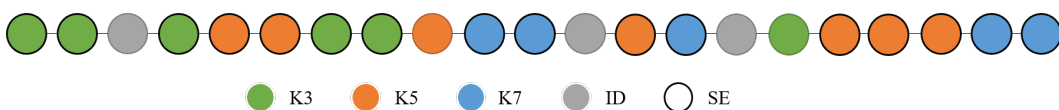
933 **Figure 4: Normalized distance matrices calculated with various methods.** (left) Distance matrix
934 calculated from output vectors (our method) ; (middle) From vector encoding ; (right) From one-hot
935 encoding. The architecture indices on leaves correspond to indices used in Pooling benchmark
936 (Roshtkhari et al., 2023).

937
938
939
940
941
942
943
944
945
946
947
948
949
950
951



952 **Figure 5: Tree branching for Pooling search space by hierarchical clustering.** The architecture
953 indices on leaves correspond to indices used in Pooling benchmark (Roshtkhari et al., 2023) (left)
954 Tree learned from output vectors (our method) ; (middle) From vector encoding ; (right) From one-hot
955 encoding.

956
957
958
959
960
961
962
963
964
965
966
967
968
969
970
971



967 **Figure 6: Visualization of found architecture for ImageNet.** Different colors correspond to various
968 kernel sizes and identity operation, while bold borders indicate SE module.
969

972
 973 Table 7: **CIFAR10 results on NAS-Bench-Macro (Su et al., 2021a)** search space with several
 974 various rewards. Relative rewards are calculated according to Su et al. (2021a). The rewards can be
 975 can be calculated on either training or validation set.

Search Structure	Metric	Reward Data	Reward Measure	Arch.	Best Acc.	Best Rank	Avg. Rank
Default Tree + Reg	rel.	train	loss	[22121222]	92.74	85	97
Learned Tree (ours)	rel.	train	loss	[22122220]	92.78	61	67
Default Tree + Reg	abs.	train	acc.	[22121210]	92.55	227	278
Learned Tree (ours)	abs.	train	acc.	[22110222]	92.56	209	301
Default Tree + Reg	rel.	val.	loss	[22222022]	92.71	98	120
Learned Tree (ours)	rel.	val.	loss	[21211220]	92.76	71	95
Default Tree + Reg	rel.	val.	acc.	[12222222]	92.92	21	112
Learned Tree (ours)	rel.	val.	acc.	[22212200]	92.94	19	67
Default Tree + Reg	abs.	val.	acc.	[22221200]	92.86	34	54
Learned Tree (ours)	abs.	val.	acc.	[22212220]	93.13	1	6

C.5 COMPLEXITY ANALYSIS

Considering N architectures in the search space, the computational complexity to build the tree for our method is determined by two factors: the complexity of inference to obtain output vectors from the pre-trained supernet ($O(N)$) and the cost of distance calculation and clustering ($O(N^2)$). The cost of inference depends on the complexity of the architectures in the search space, while the output distance calculation depends on number of output classes. Therefore, the total complexity can be estimated as $aN^2 + bN$. We estimate that our method works best for $N < 10k$ and estimate values of $a = 1e - 8$ and $b = 0.01$ for our ImageNet experiments. Therefore, the cost of inference dominates the overall cost.